Fröhlich Scattering Effects on Electron Mobility in β-Ga_2O_3 Power Devices under High Temperature

Yuehua Hong, Xuefeng Zheng, Hao Zhang, Yunlong He, Tian Zhu, Weidong Zhang, Jianfu Zhang, Xiaohua Ma, and Yue Hao*

The impact of Fröhlich scattering on β-Ga2O3 Schottky barrier diodes (SBDs) electron mobility, particularly at high temperatures, is investigated. This scat- tering is crucial due to electron–polar optical phonon interactions. Temperature- dependent I–V characteristics of a β-Ga2O3 SBD from 300 to 473 K showed significant current reduction due to electron–polar optical phonon scattering, supported by correlation with mobility profiles. Additionally, in situ temperature- dependent XPS analysis revealed a notable positive shift in core-level binding energy, attributed to heightened electron–phonon interactions. This study provides crucial insights into carrier transport mechanisms, essential for power device design and operation.

1. Introduction

β-Gallium oxide (Ga_2O_3), has emerged as a standout ultrawide bandgap semiconductor. β-Ga_2O_3 boasts exceptional material properties, including an impressive critical electric field strength of up to 8 MV cm^{-1} and an ultrawide bandgap ranging from 4.6 to 4.9 eV.[1,2] These characteristics uniquely position it for high-voltage applications and enable it to thrive in high-temperature environments.[3] An additional significant advantage of β-Ga_2O_3 lies in its capacity for precise n-type doping,[1,4] distinguishing it from other ultrawide bandgap semiconductors like AlN and diamond.[5,6] As a result, β-Ga_2O_3 has driven significant advancements in power devices, particularly Schottky barrier diodes (SBDs) and transistors.[7–12]

However, it is crucial to understand the impact of high temperatures on carrier transport properties, particularly carrier mobility, for devices operating in high temperature. While β-Ga_2O_3 power devices exhibit promising performance, a detailed understanding of scattering mechanisms and carrier transport, particularly at high temperatures, remains a subject of ongoing research. Complex phonon modes are excited in β-Ga_2O_3 due to its highly anisotropic monoclinic crystal structure, including acoustic deformation potential, ionized impurity, and neutral impurity scattering; electron–polar optical phonon scattering predominantly governs transport behavior in Ga_2O_3, particularly at room temperature.[13–16] Preliminary studies have debated the dominant scattering mechanism, whether nonpolar or polar, in electron transport within β-Ga_2O_3 at room temperature.[17–19] However, it is widely acknowledged that polar optical phonon scattering primarily limits electron mobility.[20–22] Recent literature indicates that electron–phonon interaction is expected to be the dominant factor at high temperatures, as suggested by transmission spectroscopy.[23] Additionally, it is reported that polar optical phonon scattering dominates the carrier transport at high temperature, consistent with calculated long-range interactions.[16] Furthermore, temperature-dependent Hall-effect measurements were conducted to confirm that the sole limiting mechanism for mobility at high temperatures is indeed polar optical phonon scattering.[14]

Comprehensive knowledge of the performance of β-Ga_2O_3 power devices at elevated temperatures and their impact on carrier transport is vital for device design and operation. In this work, we fabricate a β-Ga_2O_3 SBD and employ temperature-dependent I–V characteristics to assess the role of electron–polar optical phonon scattering in reducing current and limiting mobility at elevated temperatures. In situ temperature dependence of X-ray photoelectron spectroscopy (XPS) analysis in Ga_2O_3 was performed, revealing a positive shift in core-level binding energy due to enhanced electron–phonon interactions driven by phonon thermal energy. This work illuminates β-Ga_2O_3 power device performance at high temperatures, providing insights into crucial carrier transport mechanisms for device design and operation.

2. Results and Discussion

In semiconductor devices, carrier transport depends not only on the intrinsic carrier concentration but also on carrier mobility, which is affected by scattering mechanisms. In polar semiconductor, the Fröhlich scattering is particularly strong.[24] The Fröhlich scattering is one of the elementary interactions between charge carriers and lattice vibrations.[25] It involves the direct

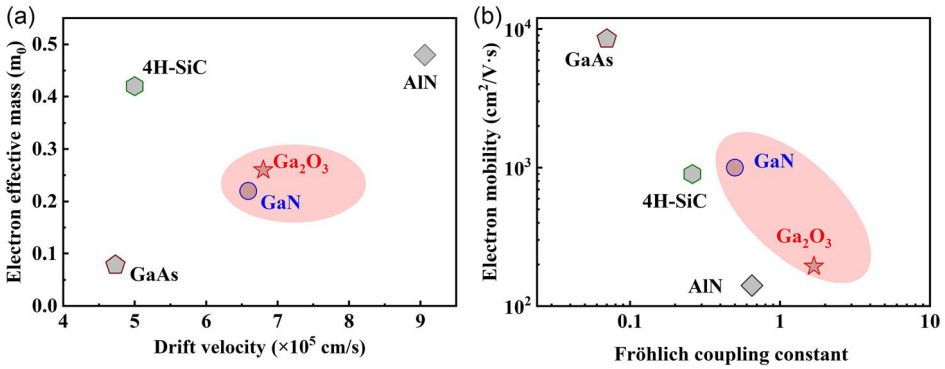

Figure 1. a) Electron effective mass versus saturation drift velocity and b) electron mobility versus Fröhlich coupling constant for various polar semiconductors at room temperature 300 K.

coupling of polar optical phonon to charge carriers, known as Fröhlich coupling. Figure 1a shows conduction band minimum (CBM) electron effective mass m^*_e for various polar semiconductors versus saturation drift velocity at 300 K.[26–33] β-Ga_2O_3 exhibits an electron-effective mass of $0.26m_0$ and a saturation drift velocity of 6.8×10^5 cm s^{-1}.[34,35] This relatively small electron-effective mass is attributed to the strong hybridization effects of Ga orbitals in the conduction band.[14] It can be seen that the electron-effective mass and saturation drift velocity of Ga_2O_3 are similar to that of GaN. However, as seen in Figure 1b, while the electron effective mass and saturation drift velocity of Ga_2O_3 are similar to GaN, the electron mobility at 300 K in unintentionally doped Ga_2O_3 (194 cm^2 V^{-1} s^{-1}) is nearly an order of magnitude lower than that of GaN bulk (1300 cm^2 V^{-1} s^{-1}).[36–38] This stark contrast in mobility can be attributed to Fröhlich scattering. The Ga—O chemical bond in Ga_2O_3 is exceptionally strong, resulting in high bond ionicity and a low phonon energy ($\hbar\omega_0$) of 29 meV.[16,39,40] This low phonon energy leads to substantial electron–polar optical phonon interaction. The dimensionless Fröhlich coupling constant,[41–45] depicted in Figure 1b, highlights that coupling in Ga_2O_3 is nearly three times stronger than that in GaN, effectively renormalizing the electron effective mass. Furthermore, the electron–phonon scattering time of Ga_2O_3 (4.5 fs) is an order of magnitude shorter than that of GaN (25 fs).[18] This can be explained by significant Fröhlich coupling. Therefore, it is imperative to emphasize the profound role of Fröhlich scattering, serving as the primary limiting factor for the diminished electron mobility observed in β-Ga_2O_3.[46]

Understanding the charge carrier transport properties and their temperature dependence is pivotal, particularly for practical device applications. Many power devices typically operate under high-temperature conditions. To thoroughly assess the performance of β-Ga_2O_3 power devices at high temperature and elucidate the impact of elevated temperatures on electron transport, we conducted a comprehensive investigation through the temperature-dependent I–V characteristics of β-Ga_2O_3 SBDs. It is vital to account for carrier concentration since impurity scattering can be a significant factor, especially when doping levels exceed 2.76×10^{18} cm^{-3}.[14] Therefore, to reduce experimental complexity, we selected a lightly doped Ga_2O_3 concentration of $\approx 1 \times 10^{16}$ cm^{-3}. Figure 2a illustrates the temperature-dependent I–V characteristics of the β-Ga_2O_3 SBD in the temperature range of 300–473 K. The inset in Figure 2 offers a cross-sectional schematic of the device structure. Notably, as the SBD is turned on, the current density decreases with increasing temperature. Current density data was collected under forward bias conditions of 2 V at each temperature, allowing the device to turn on while avoiding multiple high-field effects. As presented in Figure 2b,

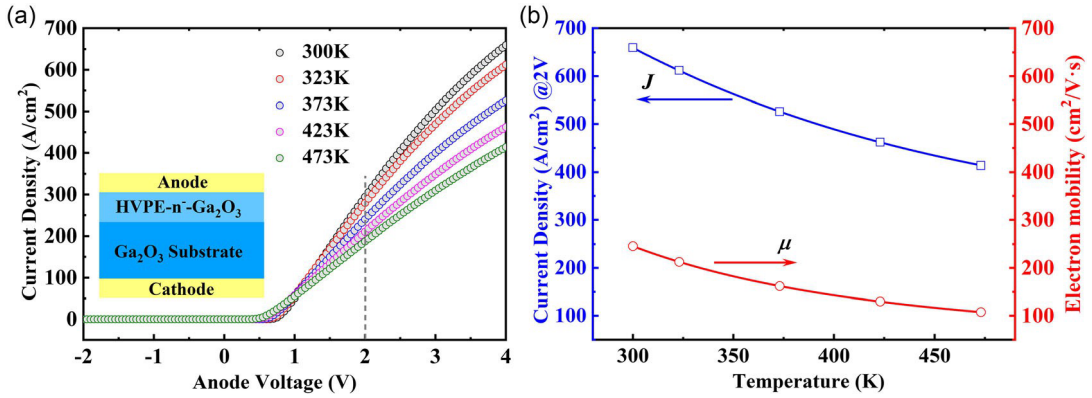

Figure 2. a) The temperature-dependent I–V characteristics of β-Ga2O3 SBD. The inset shows cross-sectional schematics of the device. b) The temperature dependence of current density extracted at 2 V and the calculated Hall-effect electron mobility at various temperatures from 300 to 473 K.

the current density at 2 V exhibits a progressive decline from 294.2 A cm^{-2} at 300 K to 187.4 A cm^{-2} at 473 K, marking a significant 36.3% reduction with rising temperature. Note that charge carrier transport properties result from a complex interplay of various scattering mechanisms. However, among diverse mechanisms, electron-polar optical phonon scattering predominantly governs transport behavior in Ga_2O_3, particularly at room temperature.[13,14] Furthermore, the prominence of electron–polar optical phonon scattering is further enhanced with increasing temperature.[16] Therefore, we hypothesize that electron–polar optical phonon scattering is the primary cause of reduced current at elevated temperatures. To validate the aforementioned hypothesis, we conducted theoretical calculations based on the following model that underscores the dominance of electron–polar optical phonon scattering in governing carrier mobility.[14]

$$\mu \propto \frac{56\ \exp(508/T) - 1}{1 + b\left(\frac{N_D}{16}\right)^{0.68}\left(T - 278\right)^{2.8}\times 10} \quad (1)$$

where μ, N_D, and T are calculated theoretically based on the model, with a doping concentration in Ga_2O_3 of $\approx 10^{16}$ cm^{-3} and a temperature range spanning from 300 to 473 K, respectively. These calculations were performed across a range of temperatures, and the calculated mobility values have been graphically represented in Figure 2b. It facilitates the examination of the temperature-dependent behavior of carrier mobility as influenced by electron–polar optical phonon scattering, revealing a significant relationship between current density and carrier mobility in β-Ga_2O_3 and providing valuable insights into the underlying physics of the system. As the temperature increases, there is a notable reduction in both the experimentally collected current density mentioned above and the calculated carrier mobility. Notably, the dynamic evolution of the calculated mobility profiles aligns closely with the experimentally collected current density data, further confirming the fidelity of our analysis. It is evident that electron–polar optical phonon scattering plays a key role in dominating carrier mobility in β-Ga_2O_3 at high temperature.

Considering that electrons interact with polar optical phonons and undergo energy absorption or emission during coupling, it can significantly impact the binding energy of electrons. In order to investigate the influence of Fröhlich coupling on electron states, XPS characteristics were conducted, which are sensitive to electronic states and binding energy. Figure 3a shows the XPS spectrum of survey for Ga_2O_3 at 300 K. It can be identified as the peak of Ga LMM, Ga2$p_{3/2}$, O1s, and O KLL, which is calibrated by C 1s peak. Figure 3b shows energy band diagram of Ga_2O_3 and core level of Ga2$p_{3/2}$. Note that the energies obtained from XPS are referenced to the Fermi level energy. For the sake of discussion, the energy derived from the valence band spectrum in XPS is measured relative to the valence band maximum (VBM) with respect to the Fermi level, denoted as a. Similarly, the binding energy of the core-level Ga2$p_{3/2}$ is referenced to the Fermi level and designated as b.

In order to investigate electron–polar optical phonon interaction at high temperature furtherly, in situ temperature dependence of XPS characteristics on Ga_2O_3 was conducted. Figure 4a shows the in situ temperature dependence of XPS characteristics on Ga_2O_3 at temperature from 300 to 473 K, whereas the VBM (a) and Ga2p core level (b) are obtained with elevated temperature. The VBM is determined by identifying the intercept between the extracted baseline and the linear extrapolation of the leading edge of the valence band. It is consistent with the estimation of the hole energy level derived from the Fermi level. Note that the electron effective mass is dependent on the electron states on CBM derived from the hybridization of Ga orbitals. Therefore, the Ga2p core levels were selected to investigate. To show the dynamic evolution qualitatively, the temperature dependence of a and b is depicted in Figure 4b. Interestingly, insignificant variations of VBM are found with increasing temperature, and it is consistently observed to be approximately 3.2 eV below the Fermi level. Note that the Fermi level actually matches with VBM.[47] Therefore, it suggests that the Fermi level experiences insignificant movement despite exposure to high temperature, aligning with stable energy band structure in Ga_2O_3 under high temperature. On the other hand, a noteworthy positive shift in the binding energy of Ga2p core levels from 1117.37 to 1117.78 eV is observed as the temperature increases from 300 to 473 K. This elevated binding energy arises from a charge transfer effect.[48,49] As the temperature increases, the interplay between electrons and phonons becomes more pronounced, driven by the heightened thermal energy carried by the phonons. This heightened energy prompts a more efficient absorption of phonon energy by electrons, triggering a consequential

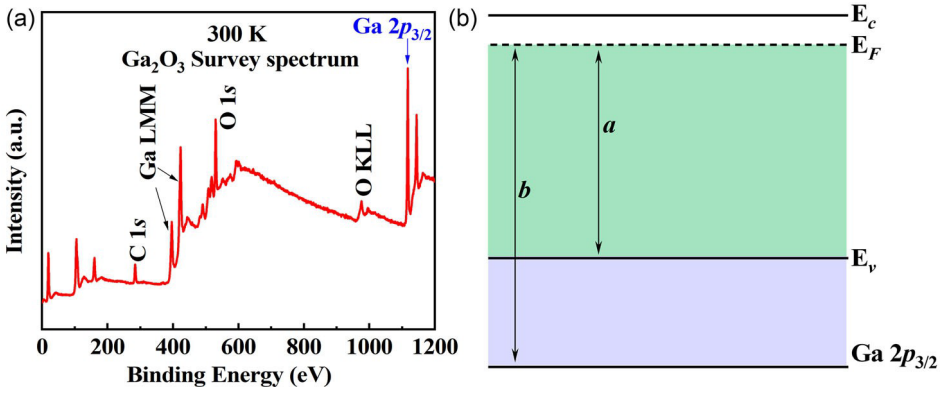

Figure 3. a) XPS spectrum of survey for Ga_2O_3 at 300 K. b) The energy band diagram of Ga_2O_3. The a and b refer to VBM and Ga 2$p_{3/2}$ core-level.

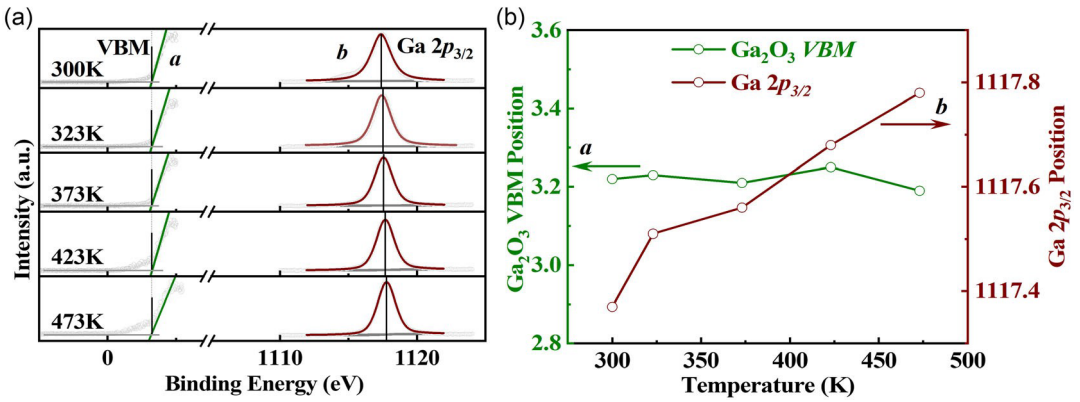

Figure 4. Temperature-dependent XPS spectrum of for Ga_2O_3 from 300 to 473 K. a) VBM a and Ga 2$p_{3/2}$ core-level b. b) The dynamic evolution of VBM and Ga 2$p_{3/2}$ core level based on the temperature from 300 to 473 K.

redistribution of electrons and instigating a charge transfer effect.[50] This phenomenon, observed in our study, serves as a critical precursor to the manifestation of the Fröhlich coupling. In essence, the heightened absorption of phonon energy by electrons, especially in the escalating temperatures as detailed in our observations, serves as a pivotal prelude to the intricate influence of Fröhlich coupling in Ga_2O_3. The ensuing adjustments in electron distribution, coupled with the consequential charge transfer effects, underscore the significant role played by Fröhlich coupling in the observed increase in binding energy. This phenomenon shares similarities with the behavior observed in ZnO.[51] To a certain extent, in our study, the temperature-dependent XPS analysis provides a unique window into the evolving nature of the electron–phonon coupling strength as temperatures vary. This analytical approach significantly bolsters the robustness of our investigation into the intricate realm of Fröhlich coupling in Ga_2O_3 at elevated temperatures.

The investigation of electron–polar optical phonon coupling, as elucidated in Figure 5, reveals a crucial interaction mechanism. Here, the de-Broglie momentum of electrons is denoted as P,[52] while the polar optical phonon energy is represented by $\hbar\omega_0$, signifying the quantized energy associated with lattice vibrations. This electron–polar optical phonon interaction mechanism is fundamentally one of the primary interactions between

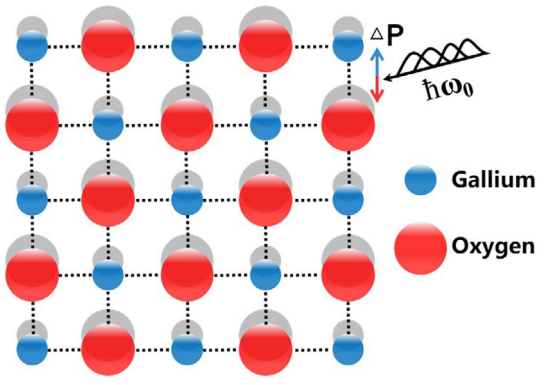

Figure 5. Schematics of the Fröhlich coupling mechanism: polar optical phonon–electron interaction.

charge carriers and lattice vibrations. Within this mechanism, polar optical phonons, carrying the distinct energy quantum of $\hbar\omega_0$, facilitate an energy exchange with electrons. Simultaneously, electrons manifest a specific de-Broglie momentum, reflecting their wave-like nature and momentum within the Ga_2O_3 material. The intricate interaction results in the absorption and emission of energy, establishing a coupling between electrons and lattice vibrations. Consequently, it assumes a pivotal role in governing charge carrier transport within Ga_2O_3, significantly influencing electron mobility.

3. Conclusion

In conclusion, our study unveils the pivotal role of the Fröhlich scattering mechanism in governing electron mobility in Ga_2O_3, particularly at high temperature. This insight holds profound implications for the field of power devices, where high-temperature operation is often a critical requirement. By fabricating a β-Ga_2O_3 SBD and conducting temperature-dependent I–V characteristics, we highlight the significance of electron–polar optical phonon scattering in reducing current at elevated temperatures. The close alignment between experimentally collected current density data and calculated mobility profiles underscores the practical relevance of the Fröhlich mechanism. Furthermore, our in situ temperature dependence of XPS analysis reveals a positive shift in core-level binding energy due to enhanced electron-phonon interactions driven by phonon thermal energy. These findings emphasize the essential role of electron–phonon interactions in Ga_2O_3 and their implications for optimizing power device performance under high-temperature conditions. This work contributes to the broader efforts in semiconductor physics and the development of high-performance electronic properties.

4. Experimental Section

A β-Ga_2O_3 SBD was fabricated on a commercial Ga_2O_3 wafer. A 10 μm-thick n-type lightly doped Ga_2O_3 drift layer was grown on a heavy doped β-Ga_2O_3 (001) substrate with a concentration of ≈1.6 × 10^{18} cm^{-3} by halide vapor phase epitaxy (HVPE) technique. The electron concentration

was determined to be 135 $cm^2 V^{-1} s^{-1}$ from Hall measurement. The cathode Ti/Au (20/200 nm) was deposited entirely on the Ga_2O_3 substrate by e-beam evaporation and subsequently subjected to Ohmic annealing at 470 °C. The circular anode Ni/Au (45/200 nm) with a radius of 60 μm was deposited on a drift Ga_2O_3 layer. The temperature-dependent *I–V* characteristics of devices were conducted with Keysight B1500A Semiconductor Device Analyzer at temperature ranging from 300 to 473 K. The in situ temperature-dependent XPS characteristics were employed to analyze the dynamic evolution of VBM and Ga $2p_{3/2}$ core-level of β-Ga_2O_3 within a temperature range of 300–473 K. We used Al K_α ($h\nu$ = 1486.6 eV) as an X-ray radiation source and calibrated the measurements with the C 1*s* peak (284.8 eV). A charge neutralizer was employed to counterbalance electrical signals, preventing positive charge accumulation due to X-ray photon excitation at the surface of sample. The XPS characteristics met an energy resolution of 0.1 eV. Therefore, the spectral shifts from XPS characteristics observed in our result were indeed larger than this resolution. This ensured that the shifts were significant and not due to the limitations of the measurement resolution.

Acknowledgements

This work was supported in part by the National Natural Science Foundation of China (grant nos. U2241220 and 61974115), in part by the National Key Research and Development Project of China (grant no. 2021YFB3602404), and by the fund of the National Innovation Center of Radiation Application (no. KFZC2022020401).

[1] S. Pearton, F. Ren, M. Tadjer, J. Kim, *J. Appl. Phys.* 2018, *124*, 220901.
[2] M. Higashiwaki, K. Sasaki, A. Kuramata, T. Masui, S. Yamakoshi, *Appl. Phys. Lett.* 2012, *100*, 013504.
[3] A. J. Green, J. Speck, G. Xing, P. Moens, F. Allerstam, K. Gumaelius, T. Neyer, A. Arias-Purdue, V. Mehrotra, A. Kuramata, *APL Mater.* 2022, *10*, 029201.
[4] M. Higashiwaki, *Phys. Status Solidi* 2021, *15*, 2100357.
[5] S. J. Pearton, J. Yang, P. H. I. V. Cary, F. Ren, J. Kim, M. J. Tadjer, M. A. Mastro, *Appl. Phys. Rev.* 2018, *5*, 011301.
[6] M. Labed, N. Sengouga, C. Venkata Prasad, M. Henini, Y. S. Rim, *Mater. Today Phys.* 2023, *36*, 101155.
[7] J. Yang, S. Ahn, F. Ren, S. J. Pearton, S. Jang, A. Kuramata, *IEEE Electron Device Lett.* 2017, *38*, 906.
[8] S. Roy, A. Bhattacharyya, C. Peterson, S. Krishnamoorthy, *IEEE Electron Device Lett.* 2022, *43*, 2037.
[9] J. W. Palmour, H. S. Kong, R. F. Davis, *J. Appl. Phys.* 1988, *64*, 2168.
[34] K. Yamaguchi, *Solid State Commun.* 2004, *131*, 739.
J. B. Varley, J. R. Weber, A. Janotti, C. G. Van de Walle, *Appl. Phys. Lett.* 2010, *97*, 142106.
[36] Z. Feng, A.F.M.A.U. Bhuiyan, Z. Xia, W. Moore, Z. Chen, J. F. McGlone, D. R. Daughton, A. R. Arehart, S. A. Ringel, S. Rajan, H. Zhao, *Phys. Status Solidi: Rapid Res. Lett.* 2020, *14*, 2000145.
[37] B. K. Ridley, B. E. Foutz, L. F. Eastman, *Phys. Rev. B* 2000, *61*, 16862.
[38] C. Hamaguchi, *J. Appl. Phys.* 2021, *130*, 125701.
[39] M. Biswas, H. Nishinaka, *APL Mater.* 2022, *10*, 060701.
[40] K. A. Mengle, E. Kioupakis, *AIP Adv.* 2019, *9*, 015313.
[41] R. Trommer, M. Cardona, *Phys. Rev. B* 1978, *17*, 1865.
[42] J. P. Nery, P. B. Allen, *Phys. Rev. B* 2016, *94*, 115135.
[43] G. Rossbach, M. Feneberg, M. Röppischer, C. Werner, N. Esser, C. Cobet, T. Meisch, K. Thonke, A. Dadgar, J. Bläsing, A. Krost, R. Goldhahn, *Phys. Rev. B* 2011, *83*, 195202.
[44] E. R. Margine, X. Blase, *Appl. Phys. Lett.* 2008, *93*, 192510.
[35]

[45] N. Ma, N. Tanen, A. Verma, Z. Guo, T. Luo, H. Xing, D. Jena, *Appl. Phys. Lett.* 2016, *109*, 212101.
[46] F. C. Correia, N. Bundaleski, O. M. Teodoro, M. Correia, L. Rebouta, A. Mendes, C. Tavares, *Appl. Surf. Sci.* 2018, *458*, 1043.
[47] M. K. Yadav, A. Mondal, S. Das, S. K. Sharma, A. Bag, *J. Alloys Compd.* 2020, *819*, 153052.
[48] H. Yang, Y. Qian, C. Zhang, D.-S. Wuu, D. N. Talwar, H.-H. Lin, J.-F. Lee, L. Wan, K. He, Z. C. Feng, *Appl. Surf. Sci.* 2019, *479*, 1246.
[49]
C. V. Ramana, E. J. Rubio, C. D. Barraza, A. Miranda Gallardo, S. McPeak, S. Kotru, J. T. Grant, *J. Appl. Phys.* 2014, *115*, 043508.
[50] C. V. Ramana, S. Roy, V. Zade, A. K. Battu, N. Makeswaran, V. Shutthanandan, *J. Phys. Chem. Solids* 2021, *157*, 110174.
[51] B.-H. Lin, H.-Y. Chen, S.-C. Tseng, J.-X. Wu, B.-Y. Chen, C.-Y. Lee, G.-C. Yin, S.-H. Chang, M.-T. Tang, W.-F. Hsieh, *Appl. Phys. Lett.* 2016, *109*, 192104.
[52] S. Ciuchi, J. Lorenzana, C. Pierleoni, *Phys. Rev. B* 2000, *62*, 4426.